Available online at www.sciencedirect.com

ScienceDirect

Defence Technology 10 (2014) 177–183

www.elsevier.com/locate/dt

Quantification of projection angle in fragment generator warhead

K.D. DHOTE [a,*], K.P.S. MURTHY [a], K.M. RAJAN [a], M.M. SUCHEENDRAN [b]

[a] *Armament Research and Development Establishment (ARDE), Dr. Homi Bhabha Road, Pashan, Pune 411021, Maharashtra, India*

[b] *Department of Aerospace Engineering, Defence Institute of Advanced Technology, Pune 411025, Maharashtra, India*

Received 24 November 2013; revised 14 April 2014; accepted 6 May 2014

Available online 20 May 2014

Abstract

Tactical Ballistic Missile (TBM) class target neutralization by the fragment spray of a Fragment Generator Warhead (FGW) calls for quantification of fragment projection angle scatter to finalize the end game engagement logic. For conventional axi-symmetric warhead, dispersion is assumed to be normal with a standard deviation of 3^0. However, such information is not available in case of FGW. Hence, a set of experiments are conducted to determine the dispersion of fragments. The experiments are conducted with a specific configuration of FGW in an identical arena to quantify the scatter and then verified its applicability to other configurations having a range of L/D and C/M ratios, and contoured fragmenting discs. From the experimental study, it is concluded that the scatter in projection angle follows normal distribution with a standard deviation of 0.75° at Chi-square significance level of 0.01($\chi^2_{0.99}$).

Keywords: Fragment generator; Fragment spatial distribution; Fragmentation warhead; Projection angle scatter

1. Introduction

In a fragment generator warhead (FGW), a fragmenting disc is integrated into one end of the cylindrical casing filled with high explosive charge. On explosion, the fragments are projected outward from the fragmenting disc, which impact on the target and cause damage. Typical advantage of FGW over conventional axi-symmetric warhead is attributed to the directional projection of fragments in a narrow beam, leading to focus a very high fragmenting mass on the target to achieve severe damage such as structural failure. However, it adds a system constraint of aligning fragment beam towards target. Its deployment against tactical ballistic missile (TBM) targets was discussed in Refs. [1,2]. Design considerations, in general, are relative velocity between the target and interceptor missiles, fuze characteristics and response time, time to go, impact obliquity, probability of target inclusion in fragment spray, trade-off for fragment mass, size, shape, spray angle and density distribution, control and guidance error effects, system limitations and response time of computation, fragment delivery mechanism, initiation system and logic. Hence, optimum design of a FGW system essentially needs quantification of the fragment dispersion to plan end game logic, ensuring that target hot spot is intercepted by the fragment cloud.

Application of flash X-ray technique to analyze fragment velocity and projection angle from a square fragmenting surface of FGW was demonstrated by Held [3]. Lixin et al. did the simulations and experiments to examine the cumulative damage to target by the concave contouring of fragmenting disc by a dense fragment generator [4]. From their study results, it is observed that the peripheral fragments do not contribute to cumulative target damage. Zlatkis et al. studied the effect of peripheral confinement of the fragmenting disc on reducing the end effects. The confinement brought down the

* Corresponding author. Tel.: +91 20 25865930; fax: +91 20 25865102.

E-mail addresses: kddhote@gmail.com (K.D. DHOTE), maheshms7@gmail.com (M.M. SUCHEENDRAN).

Peer review under responsibility of China Ordnance Society

ELSEVIER Production and hosting by Elsevier

http://dx.doi.org/10.1016/j.dt.2014.05.001

scatter in the projection angle and resulted in projecting more numbers of fragments on the target [5]. However, it adds additional mass in the system and needs a trade-off.

For a specific configuration of FGW, scatter in fragment projection angle is attributed to manufacturing deviations, expansion and breakage of fragmenting disc along with casing and fragment ballistics. The scatter in projection angle, for axi-symmetric conventional warhead, is considered to have normal distribution with standard deviation of 3° [6]. However, such information for FGW was not reported in the literature, which encouraged the authors to derive it experimentally. Accordingly, a number of trials with a specific configuration of FGW were carried out in identical experimental set-up, and the data was analyzed. It is found that the projection angle scatter follows normal distribution with a standard deviation of 0.75°. Its applicability to other configurations of flat and contoured fragmenting disc was confirmed. The range of length-to-diameter ratio (L/D) was between 0.3 and 1.6. Also, the range of explosive charge mass-to-fragmenting disc metal mass ratio (C/M) was between 0.7 and 2. We considered that the cone angle of fragmenting disc is between 160° and 190°.

2. Quantification of projection angle scatter

FGW having cylindrical explosive charge length-to-diameter ratio of 0.8 and charge mass-to-fragmenting disc metal mass ratio of 1 was subjected to performance evaluation. Its configuration details and trial set-up are shown in Fig. 1. It has a hollow cylindrical casing, closing disc and ring nut made of aluminum alloy. A fragmenting disc is integrated into one end of the casing by a ring nut. The casing is filled with cast HMX/TNT (70/30) explosive. The cylindrical booster pellet is manufactured by pressing RDX/wax (95/5) powder in a mold. The pressed booster size is ∅ 20 × 10 mm and is placed in the closing disc before integrating into the casing. An electrical detonator is provided in closing disc for initiation. A total of 97 tungsten heavy alloy (WHA) cubical fragments, each having size of 6 mm, are sandwiched between two aluminum alloy discs using iron powder mixed in resin hardener. Fragments are engraved with numbers and laid in a specific order. The typical process of fragment spall mitigation adopted in preparation of fragmenting disc is disclosed in Ref. [7], which helps to identify fragment number during soft recovery. In the experiments, more than 90% of fragments were recovered and identified. The originating location of each fragment from the fragmenting disc and its impact point on the target are correlated for scatter analysis. The laying pattern of fragments in the fragmenting disc and the recovered fragments in the experiment are also shown in Fig. 1.

Total 9 trials were conducted in an identical experimental set-up. FGW is placed on a wooden stand at mid height of particle board target, which covers projection angle full cone of 25°. Straw boards are kept behind the particle boards for soft recovery. FGW is aligned, leveled and oriented towards an aim point on target to get consistent data.

It is expected to have scatter in projection angle even for the fragments located at same radial distance on the fragmenting disc due to the variations in expansion of fragmenting disc and its breaking on explosion result in the variations in fragment acceleration dynamics and fragment ballistics. The

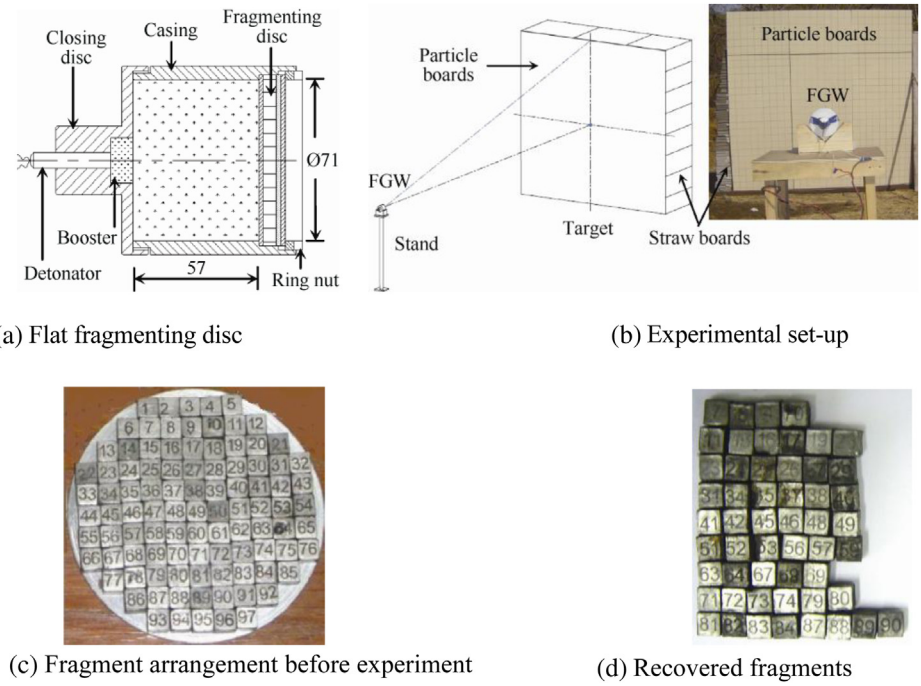

(a) Flat fragmenting disc

(b) Experimental set-up

(c) Fragment arrangement before experiment

(d) Recovered fragments

Fig. 1. FGW configuration, experimental set-up and fragment pattern along with recovered fragments.

obtained scatter in projection angle with reference to normalized radial position (ratio of fragment radial distance '*r*' to the explosive charge radius '*R*') is shown in Fig. 2. From the trial data, it is observed that the mean projection angle increases as the radial distance increases. It follows a trend line of second order equation up to 0.7*R* having statistical coefficient of determination R^2 value of 0.998, which indicates goodness of fit. The standard deviation is found to be around 0.75°. However, beyond 0.7*R*, the end effects are predominant and do not follow the trend as expected. It leads to higher projection angles and standard deviations. This effect can be reduced by providing a radial confinement as suggested by Zlatkis et al. [5]. The change in projection angle with radial position occurs due to grazing of detonation front which starts from the center of the fragmenting disc and progresses towards periphery. At radial distance beyond 0.7*R*, the lateral effects reduce the strength of detonation front interacting with the fragmenting disc. This leads to the rarefaction waves reducing the acceleration of the peripheral fragments causing the high projection angles.

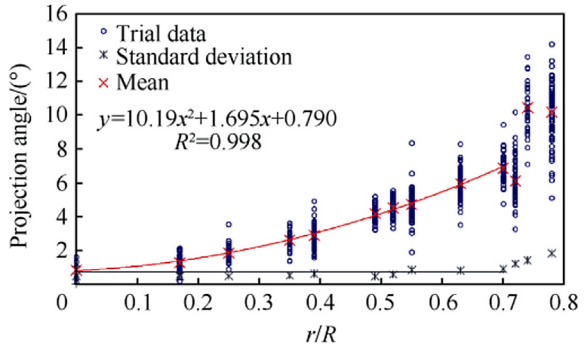

Fig. 2. Dispersion, mean and standard deviation of projection angle.

Since data up to 0.7*R* is consistent in all the trials, it is hypothesized that the dispersion follows normal distribution in each group of *r*/*R* with standard deviation of 0.75°. The goodness of fit is verified by Chi-square (χ^2) test [8]. Data at *r*/*R* = 0 was not analyzed for Chi-square since data is limited. The estimated Chi-square value is given in Table 1, where χ^2 is Chi-square; χ^2_{Critical} is the critical value of Chi-square at significance level 0.01; *r*/*R* is ratio of fragment center distance from axis to explosive charge radius, i.e. 35.5 mm; *N* is total number of fragments identified at each *r*/*R* group in 9 trials; DoF is degrees of freedom; *o* is observed frequency; *e* is expected frequency in assumed normal distribution with 0.75° standard deviation (*N*/Bins), and μ is mean projection angle in degree. The critical values at 0.01 significance level for 6 and 12 degrees of freedom (DoF) are 16.81 and 26.22, respectively, which are represented by $\chi^2_{0.99}$. Eq. (1) is used to estimate Chi-square.

$$\chi^2 = \sum_j \frac{(o_j - e_j)^2}{e_j} \tag{1}$$

For 0.17*R*, 7 bins have the angular ranges from 0° to 0.49°, 0.49°–0.87°, 0.87°–1.15°, 1.15°–1.43°, 1.43°–1.71°, 1.71°–2.09°, and 2.09° to ∞ with mean of 1.29° and standard deviation of 0.75°. The observed frequency for each bin is obtained by arranging data in ascending order, which corresponds to 2, 6, 4, 8, 7, 4 and 2 fragments in o_{Bin1}, o_{Bin2}, o_{Bin3}, o_{Bin4}, o_{Bin5}, o_{Bin6} and o_{Bin7}, respectively. This is given in Table 1. *M* and *e* in the table represent mean projection angle and expected frequency, respectively.

Table 1
Chi-square test for hypothesis of normal distribution with standard deviation of 0.75°.

	r/R								
	0.17	0.25	0.35	0.39	0.49	0.52	0.55	0.63	0.70
N	33	34	35	68	35	32	61	72	32
M	1.3	1.9	2.6	2.9	4.2	4.5	4.7	6	6.9
Bins	7	7	7	13	7	7	13	13	7
DoF	6	6	6	12	6	6	6	6	6
χ^2_{Critical}	16.81	16.81	16.81	26.22	16.81	16.81	26.22	26.22	16.81
E	4.71	4.86	5.00	5.23	5.00	4.57	4.69	5.54	4.57
o_{Bin1}	2	1	2	4	2	2	4	6	8
o_{Bin2}	6	4	4	4	4	7	5	8	7
o_{Bin3}	4	11	8	6	8	7	3	6	1
o_{Bin4}	8	5	7	4	6	2	4	6	2
o_{Bin5}	7	8	7	4	9	5	4	3	1
o_{Bin6}	4	4	4	6	5	6	8	2	3
o_{Bin7}	2	1	3	13	1	3	2	7	11
o_{Bin8}				5			4	4	
o_{Bin9}				4			11	7	
o_{Bin10}				6			7	4	
o_{Bin11}				5			3	4	
o_{Bin12}				4			4	10	
o_{Bin13}				3			2	5	
χ^2	7.1	16.2	6.4	14.6	10.4	6.5	16.8	10.3	6.5

From Table 1, it is observed that the original data of χ^2 is well below the critical value for standard deviation of 0.75°. Hence, the hypothesis that data follows normal distribution with specific mean and standard deviation in each *r*/*R* group is accepted (or at least not rejected in statistical term).

3. Verification with other FGW configurations

The applicability of standard deviation of 0.75° for other configurations is verified by varying explosive *C*/*M* ratio, *L*/*D* ratio and fragmenting disc cone angle. The flat fragmenting disc configuration is shown in Fig. 1. The contoured fragmenting disc configurations for 170° and 190° are shown in Fig. 3, along with experimental set-up used to record data in 2° interval of projection angle. The target plates having 1.5 mm thick steel are placed opposite to FGW and marked in 2° angular zones. After each trial, the number of fragment hits in each angular zone is tabulated and averaged for repeated data to generate a trend line equation based on radial distance. Radial distance for each angular zone is estimated based on an area required to pack the number of fragments in corresponding angular zone. In all the trials it is observed that projection angle follows a trend line for its radial distance of less than 0.7*R* and thereafter the projection angle increases drastically due to end effect.

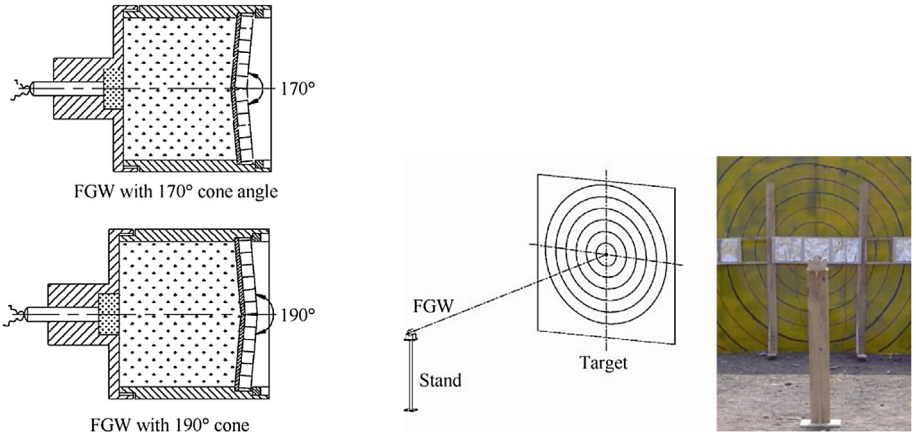

(a) Contoured fragmenting disc (b) Experimental set-up

Fig. 3. Contoured FGW configuration and experimental set-up.

3.1. FGW with flat fragmenting disc

The cylindrical explosive charges of HMX/TNT (70/30) having *L/D* 0.3 and *C/M* 0.7; *L/D* 0.4 and *C/M* 0.8; *L/D* 0.5 and *C/M* 1; *L/D* 1 and *C/M* 1; *L/D* 1.6 and *C/M* 2 are used. The details are given in Table 2, where *L/D* is length-to-diameter ratio of explosive charge; C/M is explosive Charge mass-to-fragmenting disc metal mass ratio; *D* is explosive charge diameter; TNF is total number of fragments in fragmenting disc; NoF is average number of fragments in each angular zone recorded in trial; NoT is number of trials in each configuration; and PF is packing factor which is the ratio of area of fragments packed to area of fragmenting disc, and their trend line equation is given in Fig. 4.

Table 2
Flat fragmenting disc configuration details and the number of fragments obtained in experiments with estimated *r*/R.

	L/D 0.3		*L/D* 0.4		*L/D* 0.5		*L/D* 1		*L/D* 1.6	
	C/M 0.7		*C/M* 0.8		*C/M* 1		*C/M* 1		*C/M* 2	
D/mm	148		126		114		57		71	
NoF	470		337		256		65		97	
NoT	1		1		3		3		1	
PF	0.98		0.97		0.90		0.92		0.88	
Zone	NoF	*r/R*	NoF	*r/R*	NoF	*r/R*	NoF	*r/R*	NoF	*r/R*
0°–2°	54	0.34	26	0.28	28	0.33	4	0.25	4	0.20
2°–4°	115	0.60	78	0.56	58	0.58	10	0.46	15	0.44
4°–6°	111	0.77	74	0.73	50	0.73	11	0.62	25	0.67
6°–8°	41	0.83	39	0.80	24	0.79	7	0.70	8	0.73
8°–10°	37	0.87	34	0.86	18	0.83	7	0.77	7	0.78
10°–12°	28	0.91	28	0.91	12	0.86	0	0.77	11	0.85
12°–14°	14	0.92	6	0.92	3	0.87	2	0.79	2	0.86

Based on the trend line equation, the projection angle for equal interval of 0.1*R* radial distance is estimated and given in Table 3. Sample calculation for *L/D* 0.3 and *C/M* 0.7 configuration is as follows. For $r/R = 0$, the estimated projection angle is 0.021 (i.e. 0), as shown in Fig. 4. The number of fragments projected in this direction is estimated by considering fragmenting disc area of 0.05*R*, i.e. $\pi * [0.05 * (148/2)]^2 * PF/6^2 = 1.17 \sim 1.2$. Similarly, for next *r/R* of 0.1, the number of fragments in the annular area of fragmenting disc from 0.05*R* to 0.15*R* is estimated. Accordingly, data for all the configurations is estimated.

Assuming that estimated number of fragments and projection angle for each interval of 0.1R follows a normal distribution with standard deviation of 0.75°, the spatial distribution is estimated in 2° angular zones and given in Table 4. The estimated and observed number of fragments in the angular zones of 2° intervals is compared for goodness of fit. It is observed that, in the entire configurations, the Chi-square value is less than the critical value of Chi-square for significance level of 0.01.

3.2. FGW with contoured fragmenting disc

The fragment beam can be made to converge or diverge by modifying the cone angle of fragmenting disc. To study the effect on fragment beam concentration, the FGW configurations having *L/D* 0.8 and *C/M* 1 with conical disc angles varying from 160° to 190° were tested. The fragment projection angles with reference to its radial position are shown in Fig. 5. The 160° fragmenting disc has concentrated fragment spread in 4° half cone, whereas the 190° fragmenting disc has fragment beam spray in annular half cone angle between 2° and 14°. In case of 160°, 170° and 175° cone angles, it is observed that the trend lines for the projection angles of the fragments in the region $\leq 0.4R$ are negative. However, in the process of fragmenting disc expansion starting from center, the neighboring fragments may offer resistance to have negative projection angle and these fragments are expected to move parallel to the warhead axis. To substantiate this argument,

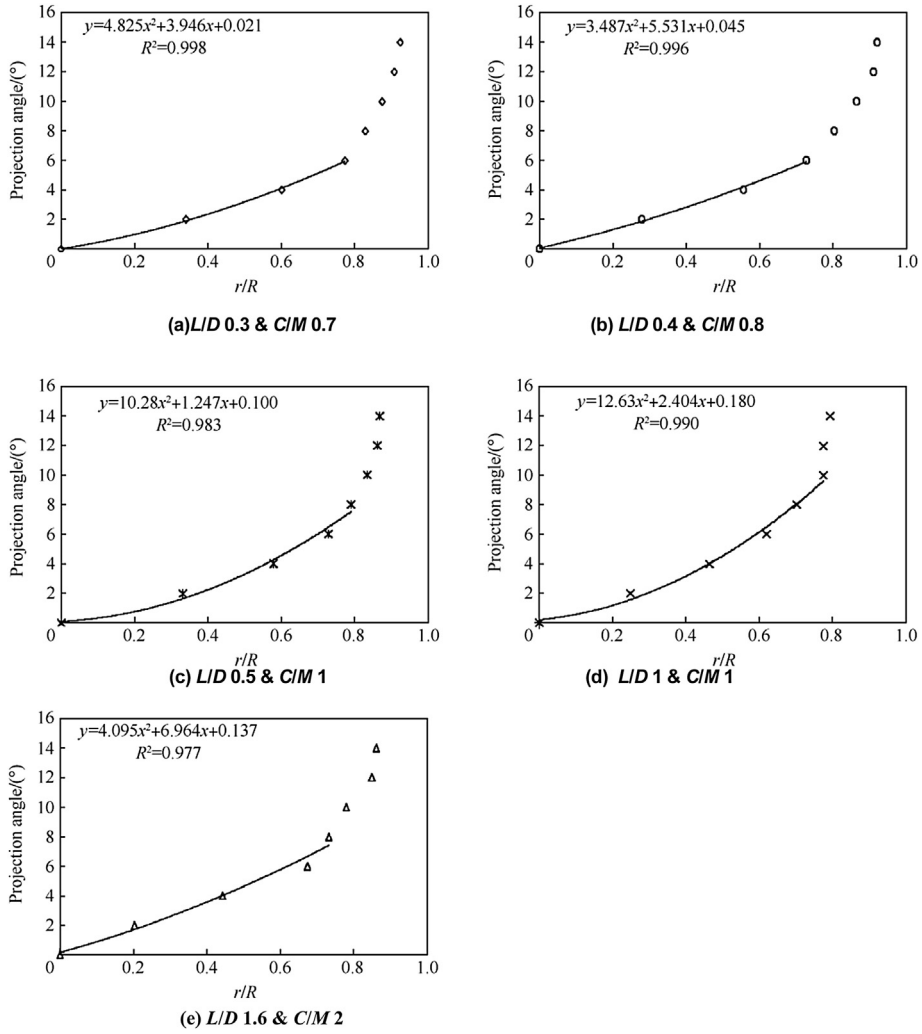

Fig. 4. Variation in projection angle with radial distance for flat fragmenting disc.

further investigation will be required. For 185° and 190° cases, the projection angles are positive and are moving away from the axis, as expected. In these configurations also, the predominance of end effect is observed for fragments originating from $r \geq 0.7$ R.

Further analysis of the data for estimated fragment number and comparison with observed data in trial are done similar to flat fragmenting disc. This is given in Tables 5−7 by considering the normal distribution with standard deviation of 0.75°. Comparing the critical Chi-square value, it is concluded that

Table 3
Projection angles (PAs) estimated from equations in Fig. 4.

	L/D 0.3 & *C/M* 0.7		*L/D* 0.4 & *C/M* 0.8		*L/D* 0.5 & *C/M* 1		*L/D* 1 & *C/M* 1		*L/D* 1.6 & *C/M* 2	
r/R	PA	NoF	PA	NoF	PA	NoF	PA	NoF	PA	NoF
0	0.0	1.2	0.0	0.8	0.1	0.6	0.2	0.2	0.1	0.2
0.1	0.5	9.4	0.6	6.7	0.3	5.1	0.5	1.3	0.9	1.9
0.2	1.0	18.7	1.3	13.4	0.8	10.2	1.2	2.6	1.7	3.9
0.3	1.6	28.1	2.0	20.2	1.4	15.3	2.0	3.9	2.6	5.8
0.4	2.4	37.5	2.8	26.9	2.2	20.4	3.2	5.2	3.6	7.7
0.5	3.2	46.8	3.7	33.6	3.3	25.5	4.5	6.5	4.6	9.7
0.6	4.1	56.2	4.6	40.3	4.5	30.6	6.2	7.8	5.8	11.6
0.7	5.1	65.6	5.6	47.0	6.0	35.7	8.1	9.1	7.0	13.5
0.8	6.3	74.9	6.7	53.8	7.7	40.8	10.2	10.4	8.3	15.5

Table 4
Chi-square test for godness of fit for flat fragmenting disc.

	L/D 0.3 & *C/M* 0.7		*L/D* 0.4 & *C/M* 0.8		*L/D* 0.5 & *C/M* 1		*L/D* 1 & *C/M* 1		*L/D* 1.6 & *C/M* 2	
Zone	*e*	*o*	*e*	*o*	*e*	*o*	*e*	*o*	*e*	*o*
0°–2°	60	54	32	26	36	28	5	4	5	4
2°–4°	101	115	65	78	43	58	8	10	13	15
4°–6°	118	111	84	74	45	50	8	11	18	25
6°–8°					45	24	9	7	21	8
8°–10°							8	7		
χ^2	2.9		4.9		17.4		2.4		11.3	
DoF	2		2		3		4		3	
$\chi^2_{Critical0.99}$	9.21		9.21		11.34		13.28		11.34	

the hypothesis of normal distribution with standard deviation of 0.75° is acceptable.

4. Conclusions

A set of experiments with FGWs having various *L/D* and *C/M* ratios were carried out. A fragmenting disc was integrated into one end of the cylindrical casing filled with explosive charge and initiated on axis from other end. In each trial, the fragment was identified by the number engraved on it and was recovered in soft medium target. The recovered fragment was correlated with its originating location in the fragmenting disc for estimation of projection angle. The projection angle data is consistent in the trials, which is characterized by using

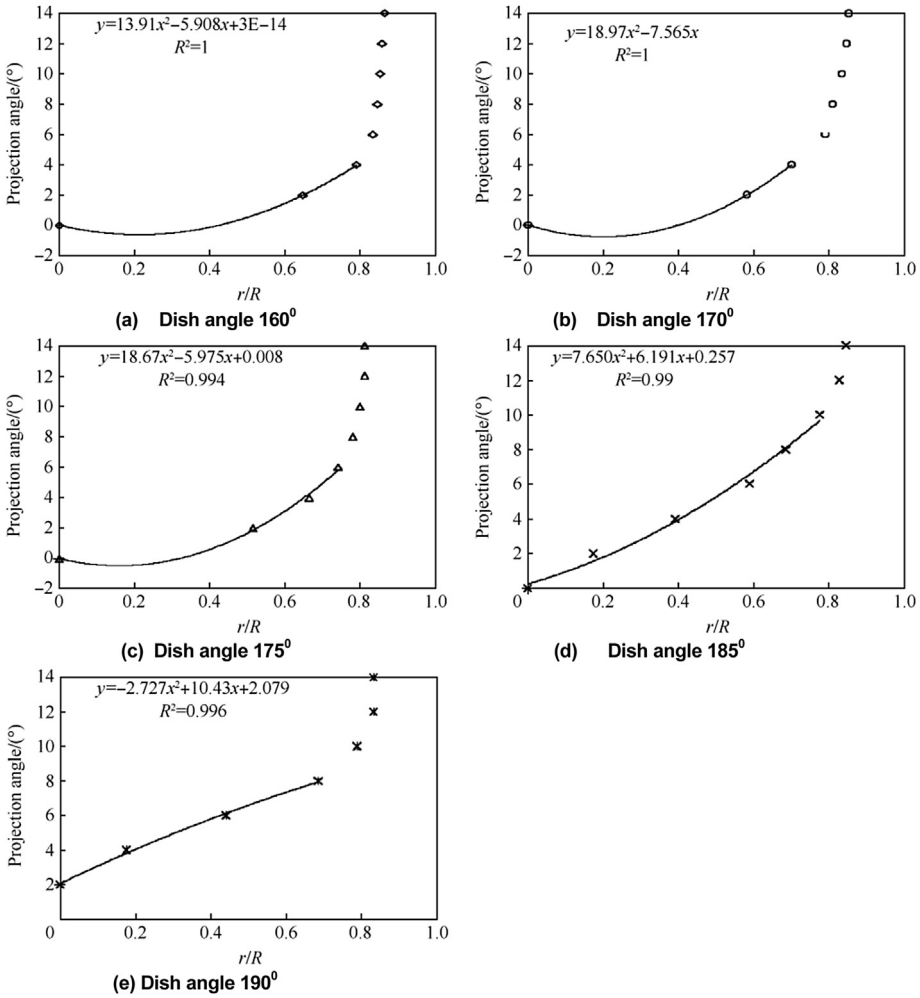

Fig. 5. Variation in projection angle with radial distance for conical fragmenting disc.

Table 5
Conical fragmenting disc configurations and the number of fragments obtained in experiments with estimated *r*/R.

	160^0		170^0		175^0		185^0		190^0	
D/mm	71		71		71		71		71	
NoF	98		98		102		98		98	
NoT	4		3		2		3		3	
PF	0.89		0.89		0.93		0.89		0.89	
Zone	NoF	*r*/*R*	NoF	*r*/*R*	NoF	*r*/*R*	NoF	*r*/*R*	NoF	*r*/*R*
0°−2°	41	0.65	33	0.58	27	0.51	3	0.17	0	0
2°−4°	20	0.79	15	0.70	18	0.66	12	0.39	3	0.17
4°−6°	7	0.83	13	0.79	11	0.74	19	0.59	16	0.44
6°−8°	2	0.85	3	0.81	6	0.78	12	0.69	27	0.69
8°−10°	1	0.85	4	0.83	3	0.80	13	0.78	15	0.79
10°−12°	1	0.86	2	0.85	2	0.81	8	0.83	7	0.83
12°−14°	1	0.86	1	0.85	0	0.81	3	0.85	0	0.83

Table 6
Projection angles (PAs) estimated from equations in Fig. 5.

	160^0		170^0		175^0		185^0		190^0	
r/*R*	PA	NoF	PA	NoF	PA	NoF	PA	NoF	PA	NoF
0.0	0.0	0.2	0.0	0.2	0.0	0.3	0.3	0.2	2.1	0.2
0.1	−0.5	2.0	−0.6	2.0	−0.4	2.0	1.0	2.0	3.1	2.0
0.2	−0.6	3.9	−0.8	3.9	−0.4	4.1	1.8	3.9	4.1	3.9
0.3	−0.5	5.9	−0.6	5.9	−0.1	6.1	2.8	5.9	5.0	5.9
0.4	−0.1	7.8	0.0	7.8	0.6	8.2	4.0	7.8	5.8	7.8
0.5	0.5	9.8	1.0	9.8	1.7	10.2	5.3	9.8	6.6	9.8
0.6	1.5	11.7	2.3	11.7	3.1	12.3	6.7	11.7	7.4	11.7
0.7	2.7	13.7	4.0	13.7	5.0	14.3	8.3	13.7	8.0	13.7
0.8	4.2	15.7	6.1	15.7	7.2	16.4	10.1	15.7	8.7	15.7

Table 7
Chi-square test for goodness of fit for conical fragmenting disc.

	160°		170°		175°		185°		190°	
Zone	*e*	*o*	*e*	*o*	*e*	*o*	*e*	*o*	*e*	*o*
0°−2°	39	41	32	33	27	27	4	3		
2°−4°	20	20	15	15	15	18	10	12	4	3
4°−6°					14	11	13	19	14	16
6°−8°							15	12	29	27
8°−10°							16	13		
χ^2	0.1		0		1.2		4.7		0.7	
DoF	1		1		2		4		3	
$\chi^2_{Critical0.99}$	6.64		6.64		9.21		13.28		16.34	

statistical Chi-square technique. It is observed that data follows normal distribution with standard deviation of 0.75°. Its applicability to other configurations of FGW with cone angles varying from 160° to 190° was verified. The variation in fragment projection angle with the fragmenting disc cone angle was also quantified. From the experimental study, it is concluded that in FGW, the projection angle scatter follows normal distribution with standard deviation of 0.75° for the fragments originating from central area of $r < 0.7R$ of explosive charge. Beyond $0.7R$, the end effects are predominant leading to higher projection angle scatter.

Acknowledgments

We are thankful to the Director, ARDE for his support for the work carried out and permitting to publish. Dr. R.S. Deodhar's guidance in statistical analysis of the data is also duly acknowledged.

References

[1] Lloyd RM. Physics of direct hit and near Miss Warhead Technologies. In: Zarchan P, editor. Progress in astronautics & aeronautics, vol. 194. American Institute of Aeronautics and Astronautics; 2001.
[2] Lloyd RM. Conventional warhead systems physics and engineering design. In: Zarchan P, editor. Progress in astronautics & aeronautics, vol. 179. American Institute of Aeronautics and Astronautics; 1998.
[3] Held M. In: Fragment generator, propellants, explosives, pyrotechnics, vol. 13; 1988. pp. 135−43.
[4] Qian LX, Qu M, Wen Y, Zhu YQ, Jiang DJ. Dense fragment generator. Propellant Explos Pyrotech 2002;27:267−78.
[5] Zlatkis A, Korin N, Gofman E. Edge effects on fragments dispersion. In: 23rd International symposium on ballistics, Tarragona, Spain; 2007.
[6] AMC Pamphlet. Research and development of material: engineering design handbook warheads-general (U), AMCP 706-290, Headquarters. Washington, D.C., USA: United States Army Material Command; 1964p.51−52.
[7] K.D. Dhote, P.N. Verma, K.P.S. Murthy. Mitigating fragment spall in fragment projector, Indian Patent Application no. 2364/MUM/2012, Armament Research and Development Establishment, DRDO, India, 2012.
[8] Spiegel MR, Stephens LJ. The Chi-square test. In: Schaum's outline series-theory and problems of statistics, McGraw-Hills, USA; 2008.